状態をどのように主観的に評価しているか（主観的幸福感など）が重要であるとの考え方が主流になってきた．

高齢者が自らの治療や生活をどのようにしたいか，自らが判断し，自らが決定するという自己決定の重要性の認識が徐々にではあるが，日本でも高まっている．医学における生命倫理の考え方はかなり浸透しており，医師が治療方針を決定し，患者が従うというパターナリズムは払拭され，高齢者が自らの治療法の選択に関与するようになってきた．

3 わが国の高齢者対策の方向

保健・医療分野における高齢者対策の一大転換が，2006年の医療制度改革関連法案の成立である．従来の高齢者対策は，1982年の老人保健法を中心に，保健と医療の総合的なサービスを提供し，基本健康診査など早期の疾病の発見，早期治療を目的として，将来の医療費増大に備えようというものであった．しかし，医療費を含め，高齢者関連の社会保障給付費が急増し，経済発展の妨げになるとの懸念から，制度全体の見直しがされた．このなかで，国と都道府県は，医療費適正化計画を策定し，生活習慣病対策や長期入院の是正など中・長期的な医療費適正化のための政策目標の策定が義務づけられた．医療分野における対策の方向は，生活習慣病予防対策としては，特定健診・保健指導の実施，在院日数の短縮のために医療機能の分化・連携の促進，在宅医療の推進，介護療養型医療施設における療養病床の転換支援などがあげられており，医療費削減が明確な目標になっている．

医療制度改革の一環として「健康保険法等の一部を改正する法律」により2008年4月からは「高齢者の医療を確保する法律」（高齢者医療確保法）として，老人保健法は廃止され，特に75歳以上の高齢者の事業については，後期高齢者医療制度（長寿医療制度）に規定されることになった．後期高齢者においては健康診査の実施は，後期高齢者医療広域連合の保健事業の一環として努力義務として課されることになり，全員が受診しなければならないという義務ではなくなった．後期高齢者を含め，高齢者では基本チェックリストなど介護予防を目的とした生活機能評価が2006年から実施されることになり，「疾病予防」より「介護予防」が中心課題であると判断されていることがうかがえる．

いずれにせよ，高齢者においても疾病や障害が発生してからの対策は後手であり，発生予防を目的とした一次予防が重要であることに変わりはない．

4 在宅ケア支援システム

高齢の患者のみならず誰でも病院や施設での生活を望む者はおらず，自宅での生活を希望していることは論を待たない．急性期や高度・先進的医療が必要な場合や，手術などを除いて，可能であれば，自宅で療養したいと考えるのは自然である．そのような患者の意思を尊重するという考え方から，在宅ケア，在宅医療は推進されてきた．しかし，現実には在宅で死亡する者の割合は減少し，現在は約8割が病院・施設死亡である．本人の療養したいところで療養できるようにする，自己決定の尊重の思想のもと，携帯型X線撮影装置や携帯型超音波診断装置の開発など，在宅での療養を可能にする医療機器の進歩がその背景にある．ただ，在宅での療養費用が病院などでの費用ほどかからないということも医療費適正化の流れのなかで強く推進されてきた要因の一つである．後期高齢者医療制度においては，地域の主治医による在宅の患者に対する日常的な医学管理から看取りまでの常時一貫した対応も診療報酬の対象になった．

高齢者が在宅で療養していくためには，主治医の理解や家族の協力があるだけでは不十分であり，在宅ケアを支える支援システムの整備が必要である．訪問看護のほか，居宅における介護サービスとして，訪問介護（ホームヘルプサービス），訪問入浴，訪問リハビリテーションなどの適切な提供が必須である．

2008年に導入された後期高齢者医療制度（長寿医療制度）については，導入直後からさまざまな意見が出されており，制度の見直しが開始された．誰もが安心して医療を受けられ，長寿を喜べる制度づくりが求められている．

〔安村誠司〕

[文献]
1）東京都老人総合研究所：サクセスフル・エイジング．東京：ワールドプランニング；1998.

介護保険

介護保険は，日本の高齢化に伴う介護問題を解決する一つの重要な制度として発足した．今では，本制度は医療と連携し，高齢者医療を実践するうえで欠かせないものになっている．制度の内容について，医師は知識をもつ必要がある．介護保険法は2000（平成12）年4月に施行され，2006（平成18）年4月に改正された．本制度は介護の社会化や，自立支援，サービスの民間化などを目的に創設された．

改正の主な内容としては，介護予防が重視され，新たな介護予防サービスの開発と普及が行われた．また，地域では地域包括支援センターが設立され，介護予防，虐待防止，地域包括ケアなどを行う多機能な地域の中核的な役割をもつ拠点が全国的に整備された．とりわけ地域における認知症の介護予防サービスは，エビデンスがさらに必要ではあるが，今後期待できるサービスである．一方，施設においてはユニットケア化，小規模多機能居宅サービスの拡充がはかられようとしている．本項では介護保険の背景とねらい，現状と実際，今後の動向について概説する．

1 介護保険の背景とそのねらい

日本が高齢化社会から超高齢社会に急速に変化し，要介護高齢者の増加に伴い，高齢者の介護問題が家庭でも社会的にも負担になり始め，制度として介護保険制度を創設する必要があった．また一方，家族の人数が減少し，家庭で介護をする環境が困難となり，介護を提供する制度として経済的にも介護保険が必要となった．

さらに高齢化に伴う医療費の負担の増加があり，新たに公的介護保険が必要となった．医療サービスのうち，いくつかが介護サービスとして転換された．日本全体でどこでもあまねく介護サービスが利用できる環境が必要であった．

福祉はこれまで措置制度が大原則であったが，公的保険制度を導入することで，措置制度から契約制度へと大きく転換された．また，主体は利用者であり，利用者の自己決定，自己選択を原則とした．また介護事業者の参入が自由化され，民間活用がねらいの一つとなった．さらに利用者の自立支援や在宅重視の原則を徹底したが，病院から在宅復帰や，医療と福祉の連携など，現実にはまださまざまな課題が存在する．制度として介護保険と自費との組み合わせ，さらにはインフォーマルケアの利用など混合介護はいうまでもないが，本制度は社会保険方式を採用し，保険料＋税財源の組み合わせ方式となっている．さらに地方分権をめざし，制度の運用は市町村単位で「給付と負担の連動」をめざしている．

2 介護保険の特徴と実際

2.1 介護保険の利用

介護サービスの利用の際には，保険者である市町村

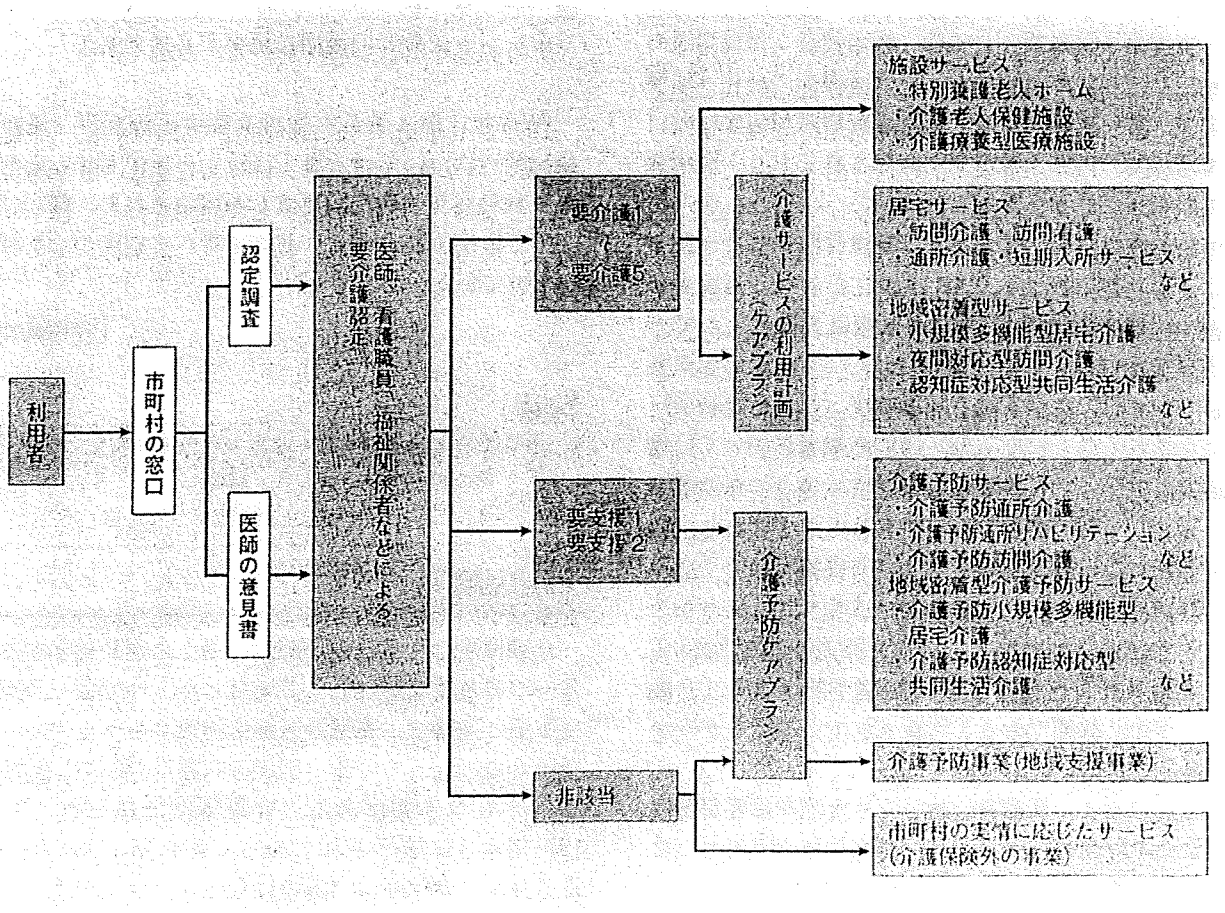

図 158 サービス利用の手続き

に申請を行う．はじめの手続きとしては認定調査を受け，主治医の意見書が必要となる．その結果を受け，各地域の介護認定審査会で検討される．その後，市町村長の名前で認定が通知される．サービスの利用の手続きの流れを図158に示した．

新しいサービスの内容を表153に示した．2006（平成18）年4月からは，これまでのデイサービスやショートステイなどの介護サービスに介護予防サービスが加わった．こうした介護サービスを利用しつつ，在宅介護を継続したり，施設を利用することになる．この点では日本における介護は量的にサービスが充実したことはいうまでもない．今後は介護は質的な向上をめざす必要がある．

また介護保険では　さらにサービス内容を担保し，本人の自己決定を支えるためにケアマネジメント制度を導入している．障害をもつ人に対して，アセスメントを行い，ケアプランを立案した後，介護サービスなどを提供し，その後モニタリングをする一連の行為を

表153　介護サービスの種類

市町村が指定・監督を行うサービス	都道府県が指定・監督を行うサービス	
地域密着型サービス 夜間対応型訪問介護 認知症対応型通所介護 小規模多機能型居宅介護 認知症対応型共同生活介護（グループホーム） 地域密着型特定施設入居者生活介護 地域密着型介護老人福祉施設入居者生活介護	居宅サービス 【訪問サービス】 訪問介護（ホームヘルプサービス） 訪問入浴介護 訪問看護 訪問リハビリテーション 居宅療養管理指導 特定施設入居者生活介護 特定福祉用具販売 【通所サービス】 通所介護（デイサービス） 通所リハビリテーション 【短期入所サービス】 短期入所生活介護（ショートステイ） 短期入所療養介護 福祉用具貸与 居宅介護支援 施設サービス 介護老人福祉施設 介護老人保健施設 介護療養型医療施設	介護給付を行うサービス
地域密着型介護予防サービス 介護予防認知症対応型通所介護 介護予防小規模多機能型居宅介護 介護予防認知症対応型共同生活介護（グループホーム） 介護予防支援	介護予防サービス 【訪問サービス】 介護予防訪問介護（ホームヘルプサービス） 介護予防訪問入浴介護 介護予防訪問看護 介護予防訪問リハビリテーション 介護予防居宅療養管理指導 介護予防特定施設入居者生活介護 特定介護予防福祉用具販売 【通所サービス】 介護予防通所介護（デイサービス） 介護予防通所リハビリテーション 【短期入所サービス】 介護予防短期入所生活介護（ショートステイ） 介護予防短期入所療養介護 介護予防福祉用具貸与	予防給付を行うサービス

ケアマネジメントという．日本の介護保険制度において，ケアマネジャーをおき，ケアマネジメントが介護サービスや施設利用において必要な制度として位置づけられた．

2.2 改正介護保険について

「2015年高齢者介護研究会」の報告をベースに，2006年に介護保険の改正がなされ，2006（平成18）年4月より改正介護保険が施行された．その趣旨は，超高齢化に突入する前の2015年に備えて，保健医療福祉の方向性を提言したものである．そこで要介護高齢者の半数が認知症をもち，介護施設入所者の8割が認知症をもつというデータに基づき，今後は身体ケアから認知症ケアに重点を移し，介護予防の重要性があることが認識された．その結果，認知症ケアの普遍化をめざすことが指摘された．その第一段階として，2004年12月に痴呆から「認知症」へ名称変更がなされた．これは疾患のイメージチェンジをすることで，認知症への理解と対応を進めることを目的とした．つまり認知症ケアの方向性として，政策的に現在検討されていることは地域包括ケアの進展であり，具体的には小規模多機能居宅介護の創設である．また地域における総合的・継続的な認知症ケア支援体制の整備として，早期発見・診断，相談体制，家族支援などが検討されており，医師は特に認知症の早期発見と診断に重要な役割を果たす必要がある．こうしたサービスのために「生活圏域」単位のサービス基盤の整備が考えられており，認知症ケアに関する人材育成（専門資格化を含む）が重要であり，高齢者虐待の防止，権利擁護システムの強化にも重点がおかれるようになっている．

2.3 地域包括支援センターの役割

改正介護保険の目玉は全国3,800か所に及ぶ地域包括支援センターの開設である．総合的な介護予防システムの確立やケアマネジメントの体系的な見直しをふまえ，地域における総合的なマネジメントを担う中核機関として創設された．専門職種として社会福祉士，保健師，主任ケアマネジャーの保健医療福祉に携わる専門職種を必置とされている．認知症や介護者もこの支援センターの直接もしくは間接的な対象となる．図159にイメージ図を示し，表154にその機能をまとめた．認知症対策に対しても地域包括支援センターは利用される．介護予防や相談支援，さらに高齢者虐待防止がその役割である．

すなわち地域包括支援センターは高齢者虐待の通報受理機関である．高齢者虐待の8割程度には認知症が

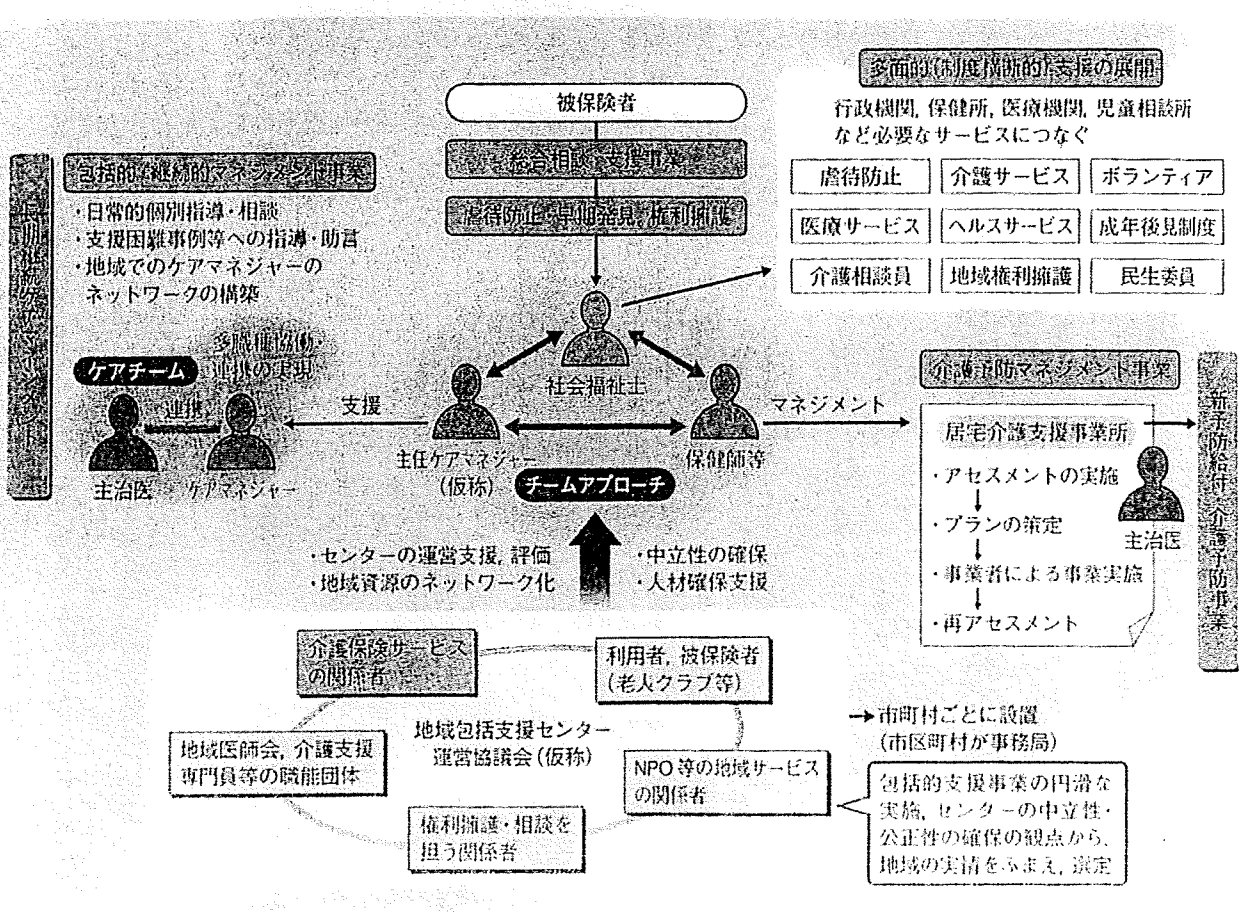

図159 地域包括支援センター（地域包括ケアシステム）のイメージ

あり，虐待を防止するための早期発見と介入を行う必要がある．そういう背景から「高齢者虐待防止・養護者支援法」が成立した．特にこの法律では介護者支援に配慮する必要を示した．医師は特に身体虐待を発見する場合があり，適切な対応を要する高齢者である．生命にかかわる高齢者虐待には通報義務がある．

24 地域密着型サービスの役割

地域密着型サービスは地域に根ざし，市町村の指定，監督を行うサービスが位置づけられた（表155）．特に小規模多機能型居宅介護サービスは在宅を1日でも長く続け，リロケーションダメージを回避することを目的とした，新しい形のサービスといえる．認知症をもつ人にとって有用な地域の認知症や独居高齢者対策サービスとして期待される．その後，有床診療所やグループホームへの住み替えが考えられている．今後は民間の高齢者賃貸住宅などの住居の拡充が予想される．

25 介護施設の変化

認知症生活介護としてのグループホームサービスの成功をふまえて，介護施設においてもユニットケア化が徐々にはかられようとしている．またユニットケア研修が必須化されている．さらに施設の地域展開が検討されており，施設のサテライト化や小規模多機能型居宅介護を行うことが計画されている．また，介護予防サービスは筋力トレーニング，口腔ケア，栄養プログラムのみが先行している．したがって，認知症の介護予防はより若い前期高齢者を対象に地域支援プログラムとして位置づけされよう．音楽療法や学習療法など種々の取り組みがなされているが，回想療法も重要な位置を占めると思われる[1]．

介護保険の改正により，各市町村の地域包括支援センターにおいて，介護予防の対象者は介護予防ケアマネジメントが提供される．すなわち介護予防プランに位置づけられ，デイサービス，デイケアをはじめ訪問リハなどが対象となる[2]．しかし質の良いサービスがなければ，介護予防の効果はない．また定年後の生き甲斐づくりの活動も認知機能の予防に役立つに違いない．戸外での活動や運動も有効であると思われる．また認知症に音楽を取り入れた運動療法を行ったところ，気分や認知機能において改善がみられた．15人の中等度から重度の患者で3か月介入をしたところ，MMSEのスコアが有意に改善した[3]．さらにバイアスロンをする人を対象とした研究で言語性短期記憶を改善することを示した報告もある[4,5]．少なくとも認知症に対するリハビリテーションを行うことで患者や家族の支援を行い，QOLの向上をはかることが重要である．さらにいえば，これらの取り組みをミニデイや宅老所などで行えば，認知症の進行遅延が可能となることを示唆しており，認知症の介護予防そのものとなる．またデイサービスやデイケアで行えば，それはアクティビティであり，より専門的に行えば，認知症の認知リハビリテーションとなる．われわれは回想療法の認知症に対する効果を検証しており，最近パソコン回想法と名づけたソフトを開発した．また認知症の個別ケアを推進するために，認知症ケアマネジメント・センター方式が開発された[6]．困難事例において有用性が示されている．

26 かかりつけ医，サポート医の研修と対応

認知症ケア支援体制の整備として，早期発見・診断，相談体制，家族支援などが検討されており，医師は特に認知症の早期発見と診断に重要な役割を果たす必要がある．真に地域医療の最大の担い手として，医師はこれまでもかかりつけ医として役割を果たしてきた．しかし，認知症は専門外として，相談や診療を避けてきた面も一部にみられた．急性期病院においても認知症の診療に困難をきたし始めている面もある．そこで，われわれは認知症（痴呆症）のクリニカルパスを作成し，病棟での診断・治療・看護の指針を作成した[7]．一方，地域では厚生労働省と医師会が協力して，国立長寿医療センターが地域の核となるサポート医の研修を開始した．サポート医はかかりつけ医研修を支援し，地域での診断や治療をチームでサポートし，認知症に

表154 地域包括支援センターの4つの機能

1. 総合的な相談窓口機能
   初期相談対応，相談支援，実態把握，権利擁護，など
2. 介護予防マネジメント
   介護予防プランの作成等の介護予防サービスの利用に要する業務
   介護予防サービスの一部実施，など
3. 包括的マネジメント（マネジメントの統括）
   市町村，関係機関との調整
   ケアマネジメント等のバックアップ，など
4. 権利擁護

表155 地域密着型サービスの種類

1. 小規模多機能型居宅介護
2. 夜間対応型訪問介護
3. 地域密着型介護老人福祉施設入所者生活介護
   （29名以下の特別養護老人ホーム）
4. 地域密着型特定施設入居者生活介護
   （29名以下の介護専用型特定施設）
5. 認知症対応型共同生活介護
   （認知症高齢者グループホーム）
6. 認知症対応型通所介護

今後の認知症対策は，早期の認定診断を出発点とした適切な対応を促進することを基本方針とし，具体的な対策として，①実態の把握，②研究開発の促進，③早期診断の推進と適切な医療の提供，④適切なケアの普及および本人・家族支援，⑤若年性認知症対策を積極的に推進する．

図 160　今後の認知症対策

なっても安心して地域で生活を継続できる体制を構築できることを計画している．今後の新しい動向として期待される．

3 今後の課題

介護保険が改正され，さまざまな課題がまた明らかになってきている．たとえば介護予防のサービスの質と量の問題，介護予防チェックリストの問題，小規模多機能型居宅介護がそれほど増加していないこと，介護療養型医療施設が転換されることなど，多くの課題がある．また若年性認知症の課題も山積している．しかしながら，最大の課題は受給者の拡大である．現在も議論が続けられているが，知的・身体・精神障害者も介護保険の対象となる可能性がある．その前途には多くの課題が存在する．すなわち介護保険制度は，改正をしながら時代のニーズに合わせてその形態を変えていくことになる．そのためには5年ごとにより良い介護保険に改正していくことになっている．その課題の一つは要介護認定の方法であり，サービスの量と質の向上である．またサービス利用者の増加に伴い，保険料が増加する．これ以上の負担は困難であると考え

られ，そのためには被保険者の年齢を40歳以上から30歳以上か20歳以上に引き下げることが最も現実的な対応である．

介護保険はもともと新たな挑戦であり，井形昭弘氏によれば，当初より「走りながら考える」とされた．つまり法律の改正を経て，継続させることが重要であり，より良い制度に変えていく必要がある．さらに認知症対策は重要な課題であり，2008（平成20）年には「認知症の医療と生活の質の向上の緊急プロジェクト」が発足し，今後の認知症対策について検討会が開催された．その内容は認知症疾患医療センターを創設すること，コールセンターをおくなど，若年性認知症対策を行うこと，疫学調査を行うこと，研究や薬剤，検査方法の開発，人材育成を行うことなどである．これらの政策により，認知症対策が前進することを期待している（図160）．

認知症のケアは現在，パーソンセンタードケアの言葉にのっとり，さまざまな取り組みがなされ始めている．介護保険制度を利用して，在宅療養を継続している認知症高齢者も多くみられる．また介護施設はケアの改善をはかり，介護者の介護負担の軽減に役立つことができる．今後，かかりつけ医，サポート医は地域での認知症の医療とケアに大きく関与することが期待される．

〔遠藤英俊〕

[文献]
1) 遠藤英俊：いつでもどこでも回想法，高齢者介護予防プログラム，東京：ごま書房；2005.
2) 鈴木憲一：介護保険制度の見直し―新予防給付を中心として，群馬県医師会報 2004；676：8.
3) Van de Winckel A, Feys H, De Weerdt W, et al：Cognitive and behavioural effects of music-based exercises in patients with dementia. *Clin Rehabil* 2004；18：253.
4) Grebot C, Groslambert A, Pernin JN, et al：Effects of exercise on perceptual estimation and short-term recall of shooting performance in a biathlon. *Percept Mot Skills* 2003；97：1107.
5) 中村重信（編著）：痴呆疾患の治療ガイドライン，東京：ワールドプランニング；2003.
6) 認知症介護研究研修センター東京センターほか（編）：認知症の人のためのケアマネジメント センター方式の使い方・活かし方，東京：認知症介護研究・研修東京センター；2005.
7) 遠藤英俊：痴呆性高齢者のクリティカルパス，名古屋：日総研；2004.

精神保健

1 精神保健と内科学

今日，精神保健（mentalhealth）の重要性が医学一般の領域で重視されているのは，①疾病動態の変化，②病因に関する説明の変化，③社会におけるストレス要因（stressor）の増加と変化，の3要因が関係している．

厚生労働省“患者調査”による年間受療統計からみた疾患別受療件数は，1972年以後今日まで一貫して第1位は高血圧，第2位は精神障害，第3位は脳血管障害である．1986年以後は悪性新生物が第4位になっている．これをストレス学説の見地からみると，高血圧，脳血管障害の発症および悪化には心理的・社会的なストレスに関係するところが大きい．精神腫瘍学（psychooncology）の視点からすれば，癌の発症および増殖に対して，全身の免疫システムの低下が関係し，それはSelyeのいう汎適応症候群の第3期である“疲憊期”（exhaustion stage）の機制に基づくとされる．さらに，社会の情報化，産業構造の変化に伴う職場の変容と技術革新，および家族構造の変化，その他の条件が人々に新たな適応努力を要求していることも，ストレス要因となっている．

1980年のアメリカ家庭医協会の調査では，アメリカの家庭医を訪れる患者の65％はストレス関連疾患であるとされている．今日の内科診療にも，また一般の健康指導でも，精神保健上の考慮が必要になってきている．

2 精神的健康の概念とその現代的特徴

2-1 精神的健康の定義

世界保健機関（WHO）の健康憲章では，「健康とは単に疾病または虚弱でないということだけではなく，身体的・精神的・社会的にも調和のとれた“よい状態”（well being）である」とされている．しかし，精神的健康とは，それがいかなる状態であろうとも，精神的な正常－異常の概念と同一視することはできない．正常（normal）と異常（abnormal）は平均概念であり，知能指数（IQ）70未満を異常（精神発達遅滞）であるとするならば，IQ 130以上もやはり異常ではある．しかし，それは適応上なんら障害を生じないので，これを精神的不健康とはしない．

精神保健学上，精神的健康の定義として，①精神的疾病がないこと，②はなはだしい不安や苦悩がないこと，③社会的規範に適応した行動ができること，④自

Human Molecular Genetics, 2010, Vol. 19, No. 1 **79–89**
doi:10.1093/hmg/ddp468
Advance Access published on October 13, 2009

Mutations in NOTCH3 cause the formation and retention of aggregates in the endoplasmic reticulum, leading to impaired cell proliferation

Keikichi Takahashi[1], Kayo Adachi[1], Kaichi Yoshizaki[1,†], Shohko Kunimoto[1], Raj N. Kalaria[2] and Atsushi Watanabe[1,*]

[1]Department of Vascular Dementia Research, National Institute for Longevity Science, National Center for Geriatrics and Gerontology, Aichi, Japan and [2]Institute for Ageing and Health, Newcastle University, Newcastle upon Tyne NE4 5PL, UK

Received May 28, 2009; Revised and Accepted October 6, 2009

Mutations in the human *NOTCH3* gene cause cerebral autosomal-dominant arteriopathy with subcortical infarcts and leukoencephalopathy (CADASIL), but the pathogenic mechanisms of the disorder remain unclear. We investigated the cytotoxic properties of mutant Notch3 using stable cell lines with inducible expression of either wild-type or two mutants p.R133C and p.C185R. We found that both mutants of Notch3 were prone to aggregation and retained in the endoplasmic reticulum (ER). The turnover rates of the mutated Notch3 proteins were strikingly slow, with half-lives greater than 6 days, whereas wild-type Notch3 was rapidly degraded, with a half-life of 0.7 days. The expression of mutant Notch3 also impaired cell proliferation compared with wild-type Notch3. In addition, cell lines expressing mutant Notch3 were more sensitive to proteasome inhibition resulting in cell death. These findings suggest that prolonged retention of mutant Notch3 aggregates in the ER decreases cell growth and increases sensitivity to other stresses. It is also possible that the aggregate-prone property of mutant Notch3 contributes to a pathogenic mechanism underlying CADASIL.

INTRODUCTION

Cerebral autosomal-dominant arteriopathy with subcortical infarcts and leukoencephalopathy (CADASIL) is the most common hereditary small vessel disease that is characterized by recurrent subcortical ischemic strokes and ultimately vascular dementia (1–5). The pathological hallmark of the disorder comprises a non-amyloid and systemic angiopathy affecting mainly small and medium-size arteries (6,7). These vascular lesions are characterized by degeneration and loss of vascular smooth muscle cells (VSMCs), as well as the abnormal accumulation of granular osmiophilic material (GOM) that is also associated with the extracellular domain of Notch3 (8). CADASIL is caused by missense mutations and small deletions in the *NOTCH3* gene located on chromosome 19p13.1–13.2 (9,10). More than 170 different mutations have been found in families of many ethnic origins (11). Because Notch3 is robustly expressed in VSMCs of the vessel wall (12), VSMCs are the primary target of the pathogenic process in CADASIL.

The *NOTCH* genes, four of which are known to exist, encode highly conserved transmembrane (TM) receptors of about 300 kDa that are involved in cell fate specification during embryonic development (13). The basic structure of the Notch receptor is common to all Notch proteins: the large extracellular domain is composed of a stretch of tandem epidermal growth factor (EGF)-like repeats involved in ligand binding, and the intracellular domain includes Ankyrin/Cdc10 repeats flanked by functional nuclear localization signal sequences. During maturation and activation,

*To whom correspondence should be addressed at: Department of Vascular Dementia Research, National Institute for Longevity Sciences, National Center for Geriatrics and Gerontology, 36-3, Gengo, Morioka, Obu city, Aichi 474-8511, Japan. Tel: +81 562462311; Fax: +81 562468438; Email: watsushi@nils.go.jp
†Present address: Division of Developmental Neuroscience, Center for Translational and Advanced Animal Research (CTAAR), Tohoku University Graduate School of Medicine, 2-1, Seiryo-machi, Aoba-ku, Sendai, Miyagi, Japan.

Notch receptors undergo at least three distinct proteolytic cleavages. Following ligand interaction, the third (S3) cleavage occurs within the TM domain close to the cytoplasmic border by γ-secretase (14), which releases the intracellular domain from the cell membrane, allowing it to translocate to the nucleus and modify the transcription of target genes (15).

Thus far, the mechanisms underlying the pathological alterations in CADASIL remain unclear. CADASIL-causing mutations result in an odd number of cysteine residues in the EGF-like repeats (10). Therefore, the formation of abnormal disulfide bridges has been thought to affect receptor trafficking, processing, specificity for ligand binding and/or signal transduction (10). It remains controversial, however, whether CADASIL mutations affect receptor trafficking and signal transduction. Recent studies have suggested that mutations located in the ligand-binding site can impair signal transduction activity, whereas neither Notch3 processing nor signaling was significantly affected by other mutations outside of the ligand-binding site (16–19). On the other hand, transgenic mice expressing mutant human Notch3 (R90C) exhibited early arterial defects in normal appearing VSMC anchorage onto the adjacent extracellular matrix and cells as well as the VSMC cytoskeleton (20). These changes were followed by the appearance of GOM deposits, suggesting that cell adhesion or the cell–matrix interaction may be affected by mutations in Notch3 and that GOM deposits are not directly involved in the early stages of VSMC abnormalities. Proteomic studies using cultivated VSMCs from a CADASIL patient also revealed differences in the expression levels of proteins involved in protein degradation and folding, indicating that mutant Notch3 causes endoplasmic reticulum (ER) stress and activates the unfolded protein response (UPR) (21). Therefore, it is plausible that mutant Notch3 instigates cytotoxic effects and induces misfolding or aggregation of proteins.

To investigate the toxic effect of mutant Notch3 in culture cells, we established Notch3-inducible human embryonic kidney (HEK) 293 cell lines using the tetracycline (Tet)-on regulatory system. Here, we report that mutants of Notch3 are more prone to form aggregates, which accumulate in the ER, and more resistant to ER-associated degradation (ERAD) than wild-type Notch3. In addition, we conclude that cells expressing mutant Notch3 exhibit impaired proliferation and increased sensitivity to proteasome inhibition resulting in cell death.

RESULTS

Preparation of stable cell lines

To study the role of mutant Notch3 in CADASIL pathogenesis, we first generated cultured human aortic smooth muscle cells (Clonetics AoSMC, Lonza) expressing either wild-type or mutant [arginine 133 to cysteine (p.R133C) or cysteine 185 to arginine (p.C185R)] human Notch3. The expression of Notch3 in VSMC, however, caused excessive cell death as early as 2 days after transfection. Therefore, we established stable HEK293 cell lines in which the expression of Notch3 was inducible using the tetracycline (Tet)-on regulatory system (T-Rex system; Invitrogen). Several cell lines were obtained and at least three cell lines for each construct were selected for subsequent experimentation on the basis of equivalent expression of Notch3 (Fig. 1). Overexpression of either wild-type Notch3 or mutant Notch3 caused a pronounced increase in the expression of the ER-resident protein-folding chaperones GRP78/BiP and ERp72 (Fig. 1). These cell lines were morphologically indistinguishable by light microscopy and exhibited similar doubling rates.

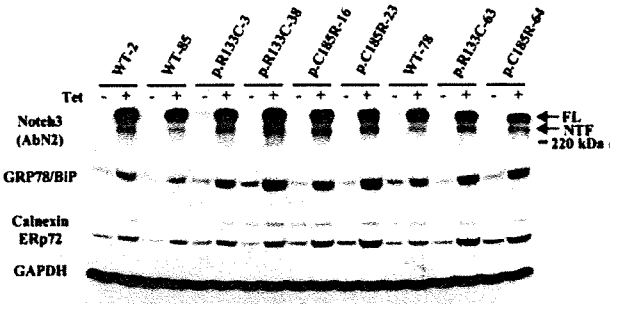

Figure 1. Expression of Notch3 in stable cells by western blot analysis. Cells were incubated with (Tet+) or without (Tet −) tetracycline (2 μg/ml) for 24 h. Cell lysates (30 μg) were prepared and subjected to SDS–gel electrophoresis. Specific proteins were detected using the relevant antibodies. The expression of Notch3 was induced by tetracycline in all cell lines. FL or NTF indicates full length or N-terminal fragment of Notch3, respectively. The same piece of membrane was probed simultaneously with Calnexin and ERp72 antibodies. The data shown are from one representative experiment for nine stable cell lines. The experiment was performed twice and similar results were obtained.

Subcellular localization of Notch3

We determined whether inducible expression of Notch3 altered the intracellular localization of mutant Notch3. The expression of either wild-type Notch3 or mutant Notch3 was induced for 24 h by tetracycline, and cells were then immunostained with Notch3 antibodies and analyzed by light microscopy. As shown in Figure 2A, mutant Notch3 tended to form dot-like aggregates in the perinuclear region of the cytoplasm, and intense immunoreactivity was detected, while only a few cells expressing with wild-type Notch3 contained the aggregates. Quantification of Notch3 immunostaining of stable cell lines revealed that nearly 50% of the mutant Notch3-expressing cells contained the intracellular aggregates. In contrast, wild-type Notch3-expressing cells containing the aggregates accounted for ~15% of the total cells (Fig. 2B).

In further analysis, we determined the precise intracellular localization of Notch3 aggregates by double-immunocytochemistry using two different ER markers (GRP78/BiP and calnexin) and a Golgi complex marker (58 K protein). In cells expressing either wild-type or mutant Notch3, most of the aggregates were colocalized with GRP78/BiP and calnexin (Fig. 3). Golgi 58 K immunoreactivity, however, was not apparent in the aggregates (Supplementary Material, Fig. S1), indicating that the Golgi complex was not involved. These observations indicated that mutant Notch3 was prone to aggregation and accumulated in the ER.

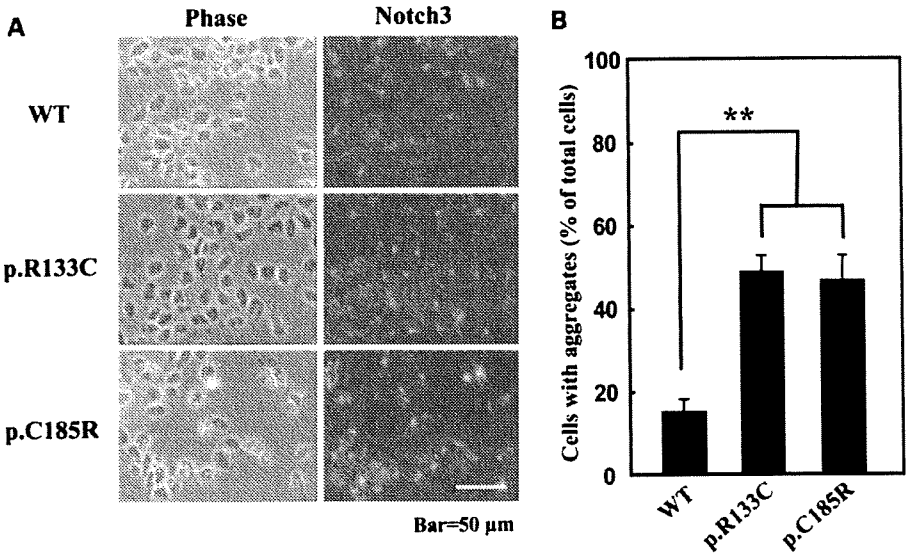

Figure 2. Immunocytochemical analysis of Notch3 in stable cells. Stable cells were treated with tetracycline (2 μg/ml) for 24 h and then stained with the anti-Notch3 antibody. (**A**) Phase contrast (left) and fluorescence (right) microscopy images were captured directly from the culture dish. This shows dot-like aggregates in the immunopositive cells. The data shown are from one representative experiment for three stable cell lines (WT-2, p.R133C-63 and p.C185R-16). The experiment was performed twice using all stable cell lines and similar results were obtained. Scale bar, 50 μm. (**B**) Cells with aggregates were quantified manually by counting cell numbers in phase contrast and immunofluorescence microscopy images and scored as the percentage of the total number of cells. Mutant Notch3 tended to form aggregates in the cytoplasm. Values represent means ± SD of data from four independent images of each stable cell line. $^{**}P < 0.01$ relative to wild-type Notch3-expressing cells.

Clearance of wild-type and mutant Notch3

The results of the immunostaining described above demonstrated that mutant Notch3 formed aggregates that are retained in the ER. Many studies have reported that mutations in proteins often cause structural alterations and result in misfolded proteins that are sequestered by ER chaperones for refolding and trafficking, before ultimately being eliminated by the ERAD system (22–28). Therefore, we determined the degradation rates of wild-type Notch3 and mutant Notch3 using pulse-chase experiments. Stable cells were treated with tetracycline for 24 h, radiolabeled for 2 h and then chased for 1–2 days in medium containing unlabeled methionine and cysteine. The labeled proteins were immunoprecipitated using an anti-Notch3 antibody. As shown in Figure 4, labeled wild-type Notch3 rapidly disappeared within 2 days and its half-life was determined to be ~0.7 days. In contrast, >70% of labeled mutant Notch3 proteins were still detectable after 2 days of chase (Fig. 4B); the half-lives of the mutants were estimated to be ~9 days for p.R133C and ~6 days for p.C185R from the slopes of the relative intensity curves. This slower degradation of mutant Notch3 was assayed by immunostaining stable cells (Fig. 5). The cells were treated with tetracycline for 24 h and then cultured in medium without tetracycline for 2 days. As expected, dot-like aggregates in the immunopositive cells of wild-type Notch3 quickly disappeared, whereas mutant aggregates did not show any discernible reduction up to 2 days. Quantitative analysis revealed that cell numbers with mutant aggregates did not appear to change for 2 days after turning off expression of the mutant Notch3. These results were confirmed by quantitative western blot analysis of stable cell lines (Supplementary Material, Fig. S2), although the amounts of mutant Notch3 (p.R133C) increased slightly at 1 day. It was also noted that wild-type Notch3 was almost entirely degraded within 2 days after arresting its expression. Thus, the aggregates of mutant Notch3 were highly resistant to degradation by the ERAD system.

Mutant Notch3 binds to ER chaperones

It has been reported that misfolded or aggregated proteins that are retained in the ER are associated with ER chaperones (22–27). We examined whether mutant Notch3 interacts with certain ER chaperones. Cell lysates were subjected to immunoprecipitation with an anti-Notch3 antibody, and the immunoprecipitated complexes were analyzed by western blotting. As shown in Figure 6, the chaperone calnexin co-immunoprecipitated with mutant Notch3 but not with wild-type Notch3, indicating that mutant Notch3 interacted exclusively with calnexin. On the other hand, GRP78/BiP co-immunoprecipitated with both the wild-type and mutant Notch3, although the amount of GRP78/BiP was higher in the mutant Notch3 immunoprecipitated samples than in the wild-type sample. The other chaperones, ERp72 and PDI, were not detected in immunoprecipitated samples of wild-type or mutant Notch3. These findings suggest that aggregation of mutant Notch3 may lead to prolonged association with calnexin, leading to retention of the aggregates in the ER.

Expression of mutant Notch3 inhibits cell proliferation

We further determined whether expression of mutant Notch3 affects cell viability. Figure 7A shows the typical growth

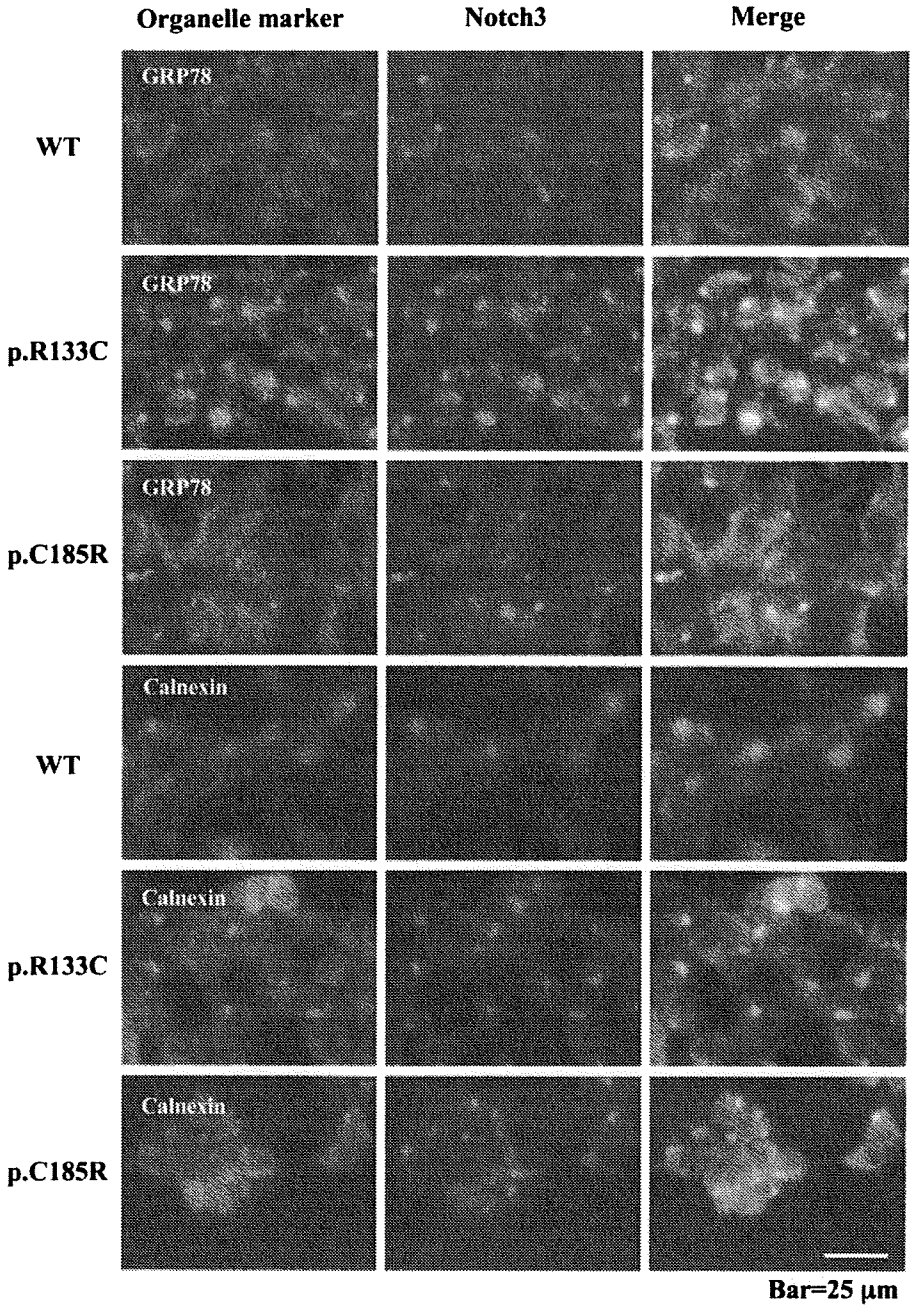

Figure 3. Subcellular localization of Notch3 aggregates. Stable cells expressing wild-type Notch3 (WT) or mutant Notch3 (p.R133C and p.C185R) were treated with tetracycline for 24 h. The cells were fixed and double-stained with antibodies. Organelle markers, GRP78/BiP and calnexin (green), were detected using primary antibodies, respectively, and visualized with either an Alexa Fluor 488-labeled secondary antibody or an FITC-labeled secondary antibody (left panels). Notch3 (red) was detected using AbN2 developed with either a Rhodamine Red-labeled secondary antibody or a Cy3-labeled secondary antibody (middle panels). The right panels represent the overlay (merge). Most of the aggregates were colocalized with GRP78/BiP and calnexin. These data shown are from representative experiments using WT-2, p.R133C-63 and p.C185R-64 cell lines for GRP78/BiP and WT-78, p.R133C-38, p.C185R-23 cell lines for calnexin, respectively. Scale bar, 25 μm.

profile as assessed by cell counting over a variable period lasting from 1 to 5 days. Expression of mutant Notch3 in tetracycline-treated cells decreased the cell number compared with that in untreated cells, whereas expression of wild-type Notch3 had relatively little overall effect on cell growth. The growth rates of cells expressing mutant Notch3 were not improved after turning off the expression of mutant Notch3 by removing tetracycline treatment (data not shown).

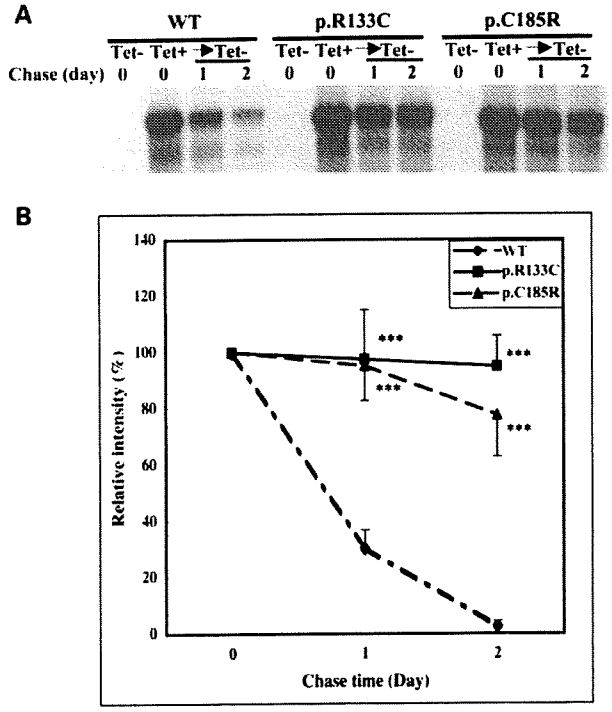

Figure 4. Efficiency and kinetics of Notch3 degradation. (**A**) Cells were treated with 2 μg/ml tetracycline for 24 h and then pulse-labeled for 2 h with L-[^{35}S]methionine and L-[^{35}S] cysteine. The labeled protein was chased for the indicated times by incubation in normal medium and then immunoprecipitated with an anti-Notch3 antibody (AbN2). The immunoprecipitates were separated on an acrylamide gel and visualized by autoradiography. The data shown are from one representative experiment for three stable cell lines (WT-2, p.R133C-3 and p.C185R-16). The experiment was performed twice using six stable cell lines (WT-2, WT-85, p.R133C-3, p.R133C-38, p.C185R-16 and p.C185R-23) and similar results were obtained. (**B**) Densitometric analysis of the autoradiograms was performed to estimate the relative amounts of wild-type Notch3 and mutant Notch3. Wild-type Notch3 rapidly disappeared within 2 days, whereas most of mutant Notch3 were still detectable after 2 days. Results represent means ± SD of data from two labeling experiments and are shown as the percentage of the material present at time 0. $^{***}P < 0.0001$ relative to wild-type Notch3.

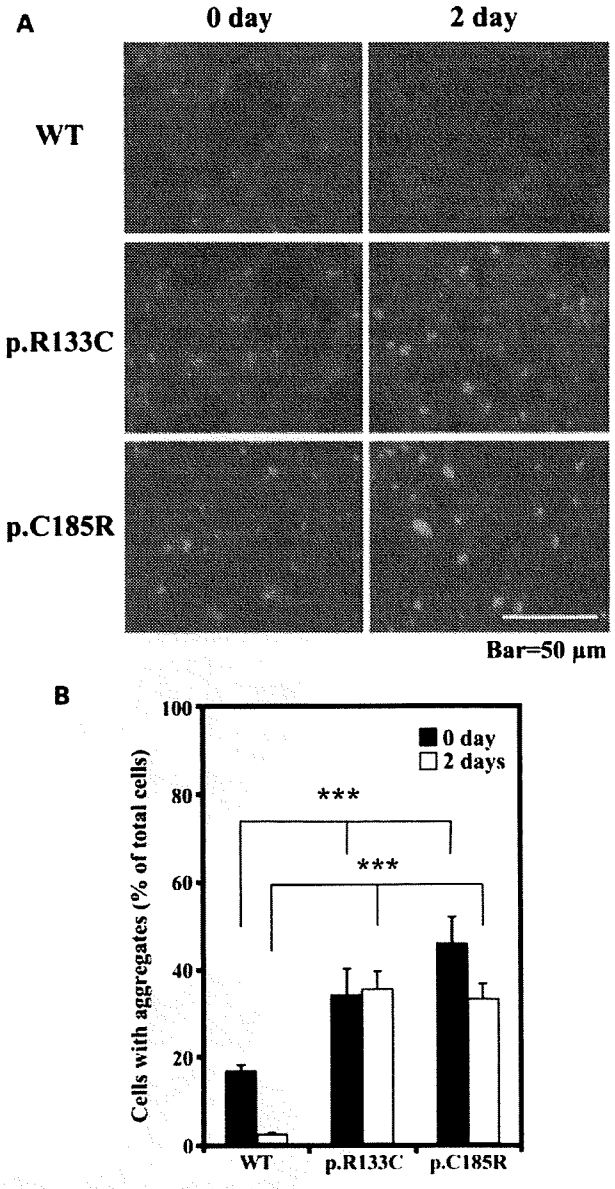

Figure 5. Retention and clearance of aggregates in cells expressing wild-type Notch3 and mutant Notch3. Cells were treated with 2 μg/ml tetracycline for 24 h and then incubated in medium without tetracycline for 2 days. (**A**) Cells were fixed at the time indicated and stained with an anti-Notch3 antibody (AbN2). The data shown represent one experiment for three stable cell lines (WT-78, p.R133C-63 and p.C185R-16). The experiment was performed twice using nine stable cell lines and similar results were obtained. Scale bar, 50 μm. (**B**) Cells with aggregates were quantified manually by counting cell numbers at the indicated times after removing tetracycline (0 days and 2 days). The aggregates of wild-type Notch3 quickly disappeared, whereas mutant aggregates did not show any discernible reduction up to 2 days. Results represent means ± SD of data from four independent images of each stable cell and are shown as the percentage of total cells counted. $^{***}P < 0.0001$ relative to wild-type Notch3-expressing cells.

These results were also confirmed in a cell proliferation assay using the WST-1 reagent (Fig. 7B and C). After 3 days of tetracycline treatment, stable cells expressing wild-type Notch3 were nearly 100% viable compared with the untreated cells, whereas cells expressing the mutant Notch3 exhibited significantly decreased viability at 33.2 and 37.8% for p.R133C and p.C185R, respectively (Fig. 7C). However, the cells expressing mutant Notch3 proteins reached confluence and did not exhibit any detectable apoptosis or other morphological abnormalities. These results suggest that expression of mutant Notch3 or aggregate accumulation decreases cell proliferation rates.

Inhibition of proteasome function increased cell death in cells expressing mutant Notch3

To determine whether apoptosis induced by impaired proteasome function depends on mutant Notch3, cell lines were treated with the proteasome inhibitor MG132 (3 μM), and cell viability was analyzed using the WST-1 assay. As shown in Figure 8A, the cells expressing mutant Notch3 were markedly sensitive to proteasome inhibition, and cell

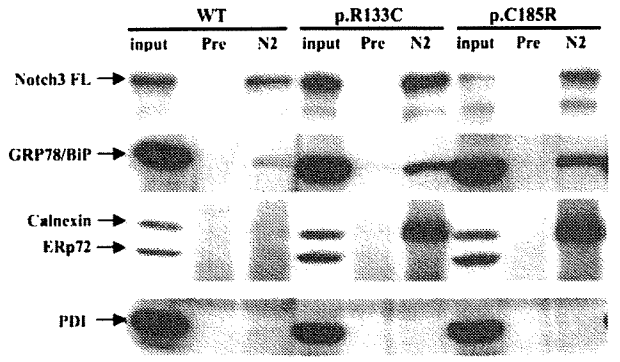

Figure 6. Identification of ER chaperones associated with mutant Notch3 by western blot analysis. Cell lysates were prepared from stable cells expressing either wild-type Notch3 or mutant Notch3 (p.R133C and p.C185R). Cell lysates (200 μg) were subjected to immunoprecipitation using an anti-Notch3 antibody (AbN2) or preimmune rabbit IgG (Pre). Immunoprecipitated complexes were subjected to SDS-PAGE, and western blot analysis was performed using mouse monoclonal antibodies against Notch3 (3A2), GRP78/BiP, calnexin, ERp72 and PDI. Total lysates (30 μg) were used as a positive control (input). The same membrane was probed simultaneously with Calnexin and ERp72 antibodies. Calnexin co-immunoprecipitated with mutant Notch3 but not with wild-type Notch3. In contrast, GRP78/BiP co-immunoprecipitated with both the wild-type and mutant Notch3. The data shown are from one representative experiment for three stable cell lines (WT-2, p.R133C-38 and p.C185R-63). The experiments were performed twice for each stable cell line with identical results.

viability was decreased by about 50% in tetracycline-treated cells compared with untreated cells. In cells expressing wild-type Notch3, there were no apparent differences in viability between tetracycline-treated and untreated cells. The effects of MG132 on cell viability are summarized in Figure 8B. These results strongly implicate that proteasome inhibition resulted in cytotoxicity associated with the accumulation of mutant Notch3.

DISCUSSION

In this study, we have shown that mutant Notch3 is more prone to form aggregates than wild-type Notch3 and that the mutant aggregates are resistant to degradation, leading to their accumulation in the ER at least in stably transfected HEK cells. The prolonged ER retention of mutant aggregates also impairs cell proliferation. A previous study reported that mouse mutant Notch3 gives rise to the increased numbers of intracellular aggregates, although the aggregates were apparently not colocalized with the markers for the ER, Golgi complex or the intermediate compartment (16). It is plausible that the modified Notch3 clone used in this study comprising chimeric receptors with insertion of the Gal4VP16 domain in the C-terminal region affected the subcellular localization of mutant Notch3. In addition, we showed that cells expressing mutant Notch3 exhibit increased sensitivity to the proteasome inhibitor MG132 resulting in cell death, which indicates that an additional stressor may be induced to disrupt cellular function. These findings suggest that impairment of ER function caused by the retention of mutant Notch3 is involved in the pathogenesis of CADASIL.

Excessive protein loading in the ER such as overexpression of either membrane proteins or secretory proteins usually induces the UPR, which is responsible for transcriptional attenuation of protein synthesis, upregulation of ER chaperones and folding enzymes to increase the capacity of the ER for protein folding and degradation (22–28). Mutations also cause aberrant folding and accumulation of the mutant protein in the ER. These unfolded proteins are retrotranslocated across the ER membrane and degraded by the ERAD process to relieve ER stress. However, some misfolded proteins are not degraded efficiently and are retained in the ER (29–33); a process which may be central to the pathogenesis of several diseases associated with ER stress. Our results showed that overexpression of wild-type Notch3 and mutant Notch3 induced the formation of aggregates in the ER, although the clearance rates of these proteins were markedly different. The aggregates of mutant Notch3 were retained in the ER and exhibited half-lives of longer than 6 days, but the aggregates of wild-type Notch3 disappeared with a half-life of less than a day. Thus, mutant Notch3 proteins form abnormal aggregates that appear trapped in the ER and are resistant to removal via the ERAD system. In contrast, the wild-type aggregates seem to be transiently formed and are readily susceptible to refolding and degradation. The biological properties that render mutant proteins prone to slower degradation remain to be identified. Because CADASIL mutations result in a free cysteine residue in the extracellular domain of Notch3, it is possible that aberrant disulfide-linking in mutant Notch3 increases the formation of aggregates and impairs the interaction with ER chaperones and proteases for efficient degradation. Recently, it has been reported that CADASIL-associated mutations significantly enhance Notch3 multimerization mediated by disulfide bonds compared with wild-type Notch3 (34). The structure of mutant Notch3 aggregates, however, may potentially be distinguished from those of wild-type aggregates by resistance to degradation, because in our experiments, wild-type Notch3 was cleared within 2 days after arresting its expression. Our preliminary experiments also revealed that both wild-type Notch3 and mutant Notch3 can be precipitated by centrifugation of cell lysates at 105 000*g* for 1 h in the presence of 1% Triton X-100 (Supplementary Material, Fig. S3), indicating that Notch3 forms a detergent-insoluble complex with a higher molecular weight. Thus, other proteins associated with the large complexes may account for the prolonged ER retention and slower degradation of mutant Notch3.

The immunoprecipitation studies suggest that calnexin only interacts with mutant Notch3. Calnexin functions as a lectin interacting with monoglucosylated oligosaccharides in folding intermediates of glycoproteins (35). Recently, it has been reported that calnexin retains misfolded proteins in membranous bodies of the ER and attenuates their degradation by the ERAD pathway (36), and overexpression of calnexin impedes trafficking of the dopamine receptor (37). Therefore, the specific interaction of mutant Notch3 with calnexin could account for the ER retention and the slower turnover rate of mutant proteins. On the other hand, CADASIL mutations have been reported to impair glycosylation of the truncated forms of Notch3 by Fringe and may induce aberrant dimerization (38). The glycosylation defects in mutant Notch3 might

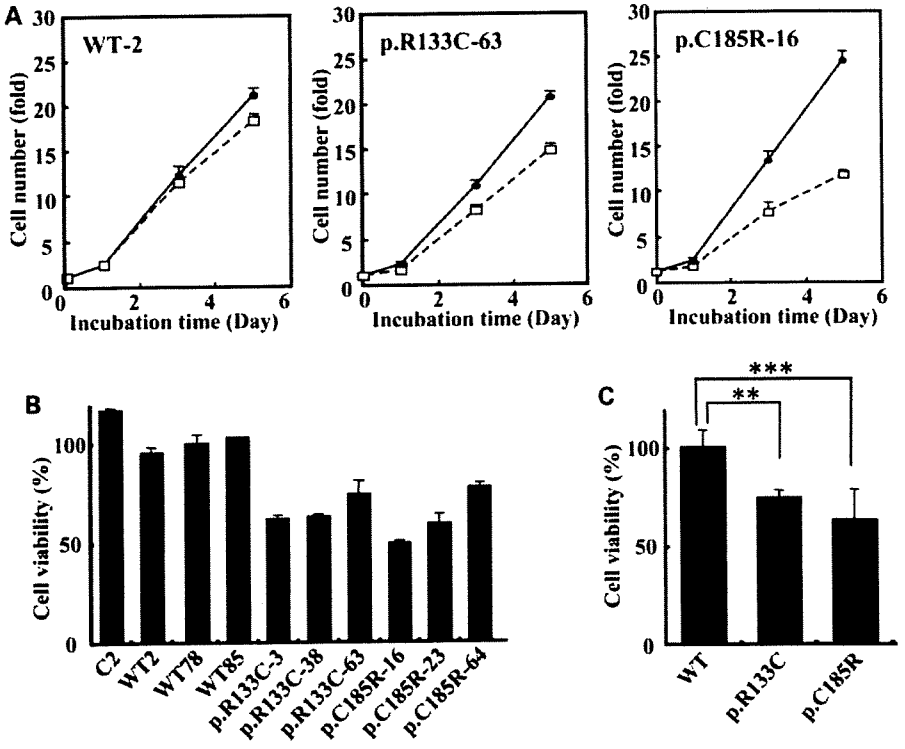

Figure 7. Comparison of proliferation rate in cells expressing either wild-type Notch3 or mutant Notch3. (**A**) Cells were incubated with (open squares) or without (closed circles) tetracycline and then harvested on days 0, 1, 3 and 5 for each of the three stable cell lines (WT-2, p.R133C-63 and p.C185R-16). Expression of mutant Notch3 decreased the cell number, whereas expression of wild-type Notch3 had relatively little overall effect on cell growth. Each data point represents the number of mean cells ± SD for triplicate counts as described in Materials and Methods. (**B**) Stable cells were incubated with or without tetracycline for 3 days. Cell viability was determined using the WST-1 reagent. C2 indicates the stable cell line transfected with empty vectors. Results represent means ± SD for triplicate wells and are shown as the percentage of the total number of cells without tetracycline treatment. (**C**) Cell viability for each cell line was converted to a percentage of the mean value relative to that of wild-type-expressing cells. Stable cells expressing wild-type Notch3 were nearly 100% viable compared with the untreated cells, whereas cells expressing the mutant Notch3 exhibited significantly decreased viability. Results represent the means ± SD of the data from different groups of cell lines (wild-type, $n = 5$; p.R133C mutant, $n = 4$; p.C185R mutant, $n = 4$). $^{**}P < 0.01$ and $^{***}P < 0.001$ relative to wild-type Notch3-expressing cells.

increase its binding affinity to calnexin compared with wild-type Notch3.

Proteasome function is essential for normal ERAD, and its inhibition causes accumulation of misfolded proteins in the ER and activates apoptotic pathways leading to cell death (39–42). Our study demonstrated that treatment with the proteasome inhibitor MG132 promoted cell death in cells expressing mutant Notch3, although cell death in cultures was not directly induced by expression of wild-type and mutant Notch3. These findings suggest that an additive effect caused by proteasome inhibition might induce apoptosis of cells with enhanced protein accumulation in the ER. It is conceivable that cells expressing mutant Notch3 develop increased sensitivity to other stress inducers such as hypoxia, oxidative stress and glucose deprivation (43–45), all of which may involve proteasome dysfunction.

Our results suggest that the cytotoxic effects of mutant Notch3 are due to its aggregate-prone property and resistance to degradation. Because all of the present experiments were performed with cultured HEK293 cells, we cannot readily extend our conclusions to *in vivo* effects of the mutation on VSMCs; however, our findings have important implications for our understanding of CADASIL pathology. First, the formation of GOM may be facilitated by the propensity for aggregation of mutant Notch3 because the extracellular domain of mutant Notch3 is a major component of GOM (8). As GOM deposits are detected around degenerating VSMCs or in the indentations of these cells, but not within the cells, it is possible that its formation occurs on the cell surface, where mutant Notch3 might act as a seed to recruit other proteins for the formation of large aggregates. It is also plausible that GOM deposits are formed in the ER and released in the extracellular space by the degeneration and disruption of VSMCs. Second, several proteins involved in protein folding and degradation have been recently reported to be upregulated in cultivated CADASIL VSMCs, suggesting that the expression of mutant Notch3 induces the UPR or impairs ERAD (21). Furthermore, disturbances in the cell surface involving cell adhesion or cell–matrix interactions might be due to impaired synthesis and transport of key membrane proteins caused by the insufficient ERAD of mutant Notch3 (20).

In summary, our study demonstrated that the intrinsic properties of mutant Notch3, which tend to form aggregates that

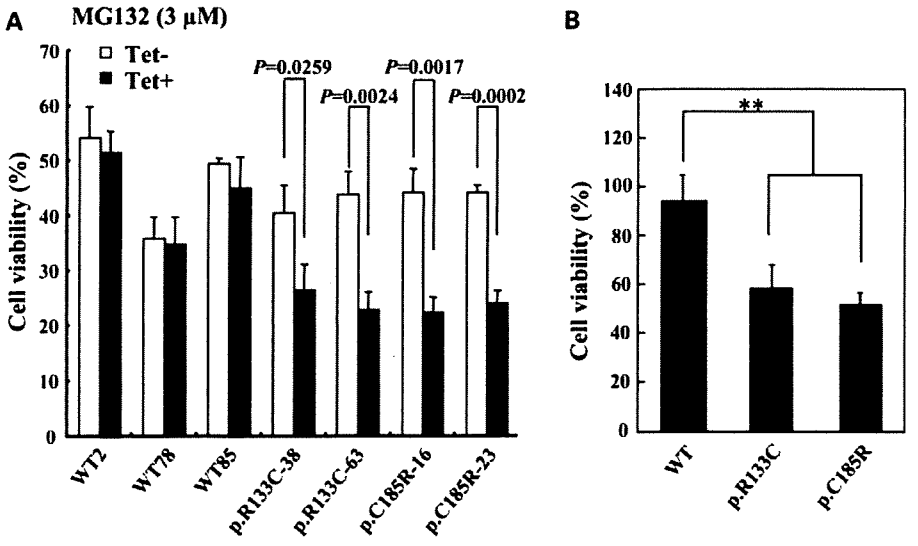

Figure 8. Different levels of sensitivity to a proteasome inhibitor. Stable cells were treated for 24 h with 3 μM MG132 in the presence (Tet+) or absence (Tet−) of tetracycline. Cell viability was determined using WST-1 reagent. (**A**) Results represent means ± SD for triplicate wells and show the percentage of the total number of cells not treated with MG132. The experiment was repeated three times using seven stable cell lines, with similar results each time. (**B**) Cell viability is summarized for cells expressing wild-type Notch3, R133C mutant Notch3 and C185R mutant Notch3, respectively. After treatment with MG132, cells expressing mutant Notch3 (Tet+) exhibited lower cell viability compared with cells not expressing Notch3 (Tet−), but cell viability was not affected by the expression of wild-type Notch3. The *y*-axis shows the percentage of the Tet+ cells to the Tet− cells exposed to MG132. Results represent means ± SD of the data. ** $P < 0.001$ relative to wild-type Notch3-expressing cells.

are resistant to the ERAD system, cause toxic effects on the proliferation of cultured cells. Further studies will be necessary to investigate the formation of mutant Notch3 aggregates in animal models and to assess their cytotoxic effects in VSMCs. Nevertheless, our findings raise the possibility that agents that inhibit the aggregation or enhance clearance of mutant Notch3 will become targets for the effective treatment or alleviation of CADASIL.

MATERIALS AND METHODS

Stable cell lines

HEK293 cells were grown in DMEM containing 10% fetal bovine serum and antibiotics. Human Notch3 cDNA (nucleotide numbers, -60-7375) was isolated from a human fetal brain cDNA library. The influenza hemagglutinin tag sequence was inserted in frame at the 3′ end of the coding region of the Notch3 cDNA. Two CADASIL mutations (p.R133C and p.C185R) in the EGF repeats were induced using a site-directed mutagenesis kit (Stratagene). The cDNAs of wild-type Notch3 and two Notch3 mutants were cloned into the *Xba*I and *Nhe*I sites of a pcDNA4/TO vector (Invitrogen) to regulate Notch3 expression using the T-Rex system (Invitrogen). All constructs were co-transfected into HEK293 cells with pcDNA/TR6 (Invitrogen) at a 1:1 ratio using an Effectene kit (Qiagen). After 48 h, cells were selected in the presence of 300 mg/ml Zeocin and 15 μg/ml blasticidin-S (Invitrogen). The expression level of Notch3 was determined by western blot analysis using an anti-Notch3 antibody (AbN2) after treatment with tetracycline (Tet; 2 μg/ml) for 48 h. The stable cell lines were maintained in DMEM containing 10% fetal bovine serum, 200 μg/ml Zeocin and 10 μg/ml blasticidin-S. The C2 clone was the stable cell line transfected with empty vectors.

Preparation of anti-Notch3 antibodies

Two rabbit polyclonal anti-human Notch3 antibodies (AbN2 and AbC2) were raised against glutathione-*S*-transferase fusion proteins containing amino acid residues 1497–1624 and 2261–2321 from the human Notch3, respectively (19). Monoclonal antibody 3A2 was raised against a synthetic peptide containing amino acid residues 1524–1538.

Western blot analysis

Cells were harvested and lysed in solution A containing 1% Triton X-100, 0.1 M Tris–HCl, pH 7.4, 0.15 M NaCl and a protease inhibitor cocktail (Boehringer Mannheim) as previously described (19). Lysates (30 μg/lane) were separated on a 7–10% SDS gel, and the separated proteins were transferred to a nitrocellulose membrane (Bio-Rad). The membrane was blocked in TBST (10 mM Tris–HCl, pH 7.4, 150 mM NaCl, 0.1% Tween-20) containing 5% non-fat milk and probed with the primary antibodies namely anti-human Notch3 (AbN2 and AbC2), anti-GAPDH (Sigma) and mouse monoclonal antibodies in a Chaperone Sampler kit (BD Biosciences), including anti-GRP78/BiP, anti-calnexin, anti-ERp72 and anti-PDI (protein disulfide isomerase). Immunoreactive proteins were detected by Western Lightning chemiluminescence reagents (Perkin Elmer). Protein concentrations were determined using the micro-BCA assay (Pierce).

Immunocytochemistry

Cells were cultured in 35 mm Petri dishes coated with poly-L-lysine and fixed in 4% paraformaldehyde in PBS at 4°C for 10 min. After treatment with 0.2% Triton X-100 for 10 min, cells were blocked with PBS containing 3% fetal bovine serum for 30 min and incubated for 1 h with the following primary antibodies at room temperature: a rabbit anti-human Notch3 (AbN2) (1 μg/ml), a goat anti-GRP78/BiP (C-20) antibody (Santa Cruz Biotechnology, diluted 1:100), a mouse anti-calnexin antibody (BD Biosciences, diluted 1:100) and a mouse anti-Golgi 58K protein antibody (Sigma, diluted 1:100). For the negative control, we used normal IgG instead of the primary antibody. Cells were washed three times with PBS and incubated for 1 h with the appropriate secondary antibodies including an Alexa Fluor 488-labeled goat anti-mouse antibody, a Rhodamine Red-labeled goat anti-rabbit antibody (Molecular Probes), an FITC-labeled donkey anti-goat antibody and a Cy3-labeled donkey anti-rabbit antibody (Chemicon) at a 1:1000 dilution in PBS. After three washes in PBS, cells were counterstained with DAPI (4′,6′-diamino-2-phenylindole, Molecular Probes) (5 μg/ml, 5 min), washed in PBS and examined under a light microscope (Olympus).

Pulse-chase analysis

Cells (1.2×10^6) were incubated for 24 h in 6-well plates coated with poly-L-lysine and treated with 2 μg/ml tetracycline for 24 h. The cells were then starved for 3 h in cysteine/methionine-free DMEM (Invitrogen) supplemented with 1% L-glutamine and 10% dialyzed fetal bovine serum and labeled for 2 h by the addition of 0.1 mCi/ml Pro-Mix L-[^{35}S] *in vitro* labeling mix (GE Healthcare). The culture medium was changed to fresh medium containing cold cysteine and methionine and chased for the indicated times. At each time point, cells were harvested and lysed in solution A (described above). The cell lysates were immunoprecipitated with anti-Notch3 (AbN2), and immunocomplexes were subjected to SDS polyacrylamide gel electrophoresis as described above. The separated proteins were visualized by fluorography using the Amplify Fluorographic Reagent (GE Healthcare) and X-ray film (GE Healthcare).

Immunoprecipitation

Cells were harvested and lysed in solution A. The lysates (200 μg of protein) were precleared with a protein G-agarose bead slurry (Boehringer Mannheim) for 1 h at 4°C and incubated at 4°C for 24 h with 3 μl of AbN2 antibodies (1 mg/ml). Immunocomplexes were pulled down with protein G-agarose beads and washed three times with RIPA buffer (1% Triton X-100, 20 mM Tris–HCl, pH 7.5, 1% deoxycholate, 0.2% SDS, 0.15 M NaCl and a protease inhibitor cocktail). After addition of the gel loading solution with 10% β-mercaptoethanol and boiling for 3 min, samples were loaded on a 7% SDS–PAGE gel. Proteins were transferred to membranes and blotted with Notch3 and several chaperone proteins antibodies as described above. The immunoreactive proteins were detected by chemiluminescence as described above.

Comparison of cell proliferation rate

Stable cells (2×10^4) were seeded in the 24-well plates and treated with or without 2 μg/ml tetracycline for the indicated times at 0 (before treatment), 1, 3, 5 days (after treatment). To determine the numbers of proliferating cells at each time point and under each condition (with or without Tet), we separately harvested cells from three wells. Then, cells in each well were stained with Trypan Blue and counted four times. Data were obtained from three independent experiments, and a plot was expressed as the mean values ± SD ($n = 3$, from three wells).

Measurement of cell viability and induction of ER stress

Stable cells (5×10^5) were seeded in 6-well plates. After 24 h, cells were incubated in fresh medium containing 2 μg/ml tetracycline for 24 h and then harvested for western blot analysis. To assess cell growth rates, stable cells (2×10^4) were seeded in 24-well plates and treated with or without 2 μg/ml tetracycline for the indicated times. Cell growth was determined by two methods: by counting in Trypan Blue solution and by means of a cell proliferation assay using the WST-1 reagent (Cell proliferation assay kit, Chemicon). This kit was used for rapid and sensitive quantification of cell proliferation and viability. The assay is based on the cleavage of the tetrazolium salt WST-1 to formazan by cellular mitochondrial dehydrogenases. To assess the effect of the proteasome inhibitor MG132 (Calbiochem), cells (2×10^4) were seeded in 24-well plates coated with poly-L-lysine. After 24 h, cells were treated with MG132 (3 μM) for 24 h in the presence or absence of tetracycline, and cell viability was determined using the WST-1 reagent.

Statistical analysis

Data are presented as means ± SD. Statistical analysis was performed using unpaired *t*-test (two-tailed) or one-way ANOVA with Dunnett's multiple comparison post hoc test (PRISM version 5.0a; GraphPad Software, La Jolla, CA, USA). Values of $P < 0.05$ were considered significant.

SUPPLEMENTARY MATERIAL

Supplementary Material is available at *HMG* online.

ACKNOWLEDGEMENTS

We thank Ms Aki Nagasaki and Ms Mikiko Matsuzaki for excellent technical assistance.

Conflict of Interest statement. None declared.

FUNDING

This work was supported by the Program for Promotion of Fundamental Studies in Health Science of the National Institute of Biomedical Innovation (NIBIO), a Research Grant for Longevity Sciences (18C-4 to K.T.) from the Ministry of Health, Labour and Welfare and the Medical Research

Council, UK programme project (G0500247) on dementia after stroke.

REFERENCES

1. Tournier-Lasserve, E., Joutel, A., Melki, J., Weissenbach, J., Lathrop, G.M., Chabriat, H., Mas, J.L., Cabanis, E.A., Baudrimont, M., Maciazek, J. *et al.* (1993) Cerebral autosomal dominant arteriopathy with subcortical infarcts and leukoencephalopathy maps to chromosome 19q12. *Nat. Genet.*, **3**, 256–259.
2. Chabriat, H., Vahedi, K., Iba-Zizen, M.T., Joutel, A., Nibbio, A., Nagy, T.G., Krebs, M.O., Julien, J., Dubois, B., Ducrocq, X. *et al.* (1995) Clinical spectrum of CADASIL: a study of 7 families. Cerebral autosomal dominant arteriopathy with subcortical infarcts and leukoencephalopathy. *Lancet*, **346**, 934–939.
3. Ruchoux, M.M. and Maurage, C.A. (1997) CADASIL: Cerebral autosomal dominant arteriopathy with subcortical infarcts and leukoencephalopathy. *J. Neuropathol. Exp. Neurol.*, **56**, 947–964.
4. Dichgans, M., Mayer, M., Uttner, I., Brüning, R., Müller-Höcker, J., Rungger, G., Ebke, M., Klockgether, T. and Gasser, T. (1998) The phenotypic spectrum of CADASIL: clinical findings in 102 cases. *Ann. Neurol.*, **44**, 731–739.
5. Kalaria, R.N., Low, W.C., Oakley, A.E., Slade, J.Y., Ince, P.G., Morris, C.M. and Mizuno, T. (2002) CADASIL and genetics of cerebral ischaemia. *J. Neural. Transm. Suppl.*, **63**, 75–90.
6. Ruchoux, M.M., Chabriat, H., Bousser, M.G., Baudrimont, M. and Tournier-Lasserve, E. (1994) Presence of ultrastructural arterial lesions in muscle and skin vessels of patients with CADASIL. *Stroke*, **25**, 2291–2292.
7. Schröder, J.M., Sellhaus, B. and Jörg, J. (1995) Identification of the characteristic vascular changes in a sural nerve biopsy of a case with cerebral autosomal dominant arteriopathy with subcortical infarcts and leukoencephalopathy (CADASIL). *Acta Neuropathol.*, **89**, 116–121.
8. Ishiko, A., Shimizu, A., Nagata, E., Takahashi, K., Tabira, T. and Suzuki, N. (2006) Notch3 ectodomain is a major component of granular osmiophilic material (GOM) in CADASIL. *Acta Neuropathol.*, **112**, 333–339.
9. Joutel, A., Corpechot, C., Ducros, A., Vahedi, K., Chabriat, H., Mouton, P., Alamowitch, S., Domenga, V., Cécillion, M., Maréchal, E. *et al.* (1996) Notch3 mutations in CADASIL, a hereditary adult-onset condition causing stroke and dementia. *Nature*, **383**, 707–710.
10. Joutel, A., Vahedi, K., Corpechot, C., Troesch, A., Chabriat, H., Vayssière, C., Cruaud, C., Maciazek, J., Weissenbach, J., Bousser, M.G. *et al.* (1997) Strong clustering and stereotyped nature of Notch3 mutations in CADASIL patients. *Lancet*, **350**, 1511–1515.
11. Tikka, S., Mykkänen, K., Ruchoux, M.M., Bergholm, R., Junna, M., Pöyhönen, M., Yki-Järvinen, H., Joutel, A., Viitanen, M., Baumann, M. *et al.* (2009) Congruence between NOTCH3 mutations and GOM in 131 CADASIL patients. *Brain*, **132**, 933–939.
12. Joutel, A., Andreux, F., Gaulis, S., Domenga, V., Cécillon, M., Battail, N., Piga, N., Chapon, F., Godfrain, C. and Tournier-Lasserve, E. (2000) The ectodomain of the Notch3 receptor accumulates within the cerebrovasculature of CADASIL patients. *J. Clin. Invest.*, **105**, 597–605.
13. Artavanis-Tsakonas, S., Rand, M.D. and Lake, R.J. (1999) Notch signaling: cell fate control and signal integration in development. *Science*, **284**, 770–776.
14. De Strooper, B., Annaert, W., Cupers, P., Saftig, P., Craessaerts, K., Mumm, J.S., Schroeter, E.H., Schrijvers, V., Wolfe, M.S., Ray, W.J. *et al.* (1999) A presenilin-1-dependent γ-secretase-like protease mediates release of Notch intracellular domain. *Nature*, **398**, 518–522.
15. Struhl, G. and Adachi, A. (1998) Nuclear access and action of notch *in vivo*. *Cell*, **93**, 649–660.
16. Karlström, H., Beatus, P., Dannaeus, K., Chapman, G., Lendahl, U. and Lundkvist, J. (2002) A CADASIL-mutated Notch 3 receptor exhibits impaired intracellular trafficking and maturation but normal ligand-induced signaling. *Proc. Natl Acad. Sci. USA*, **99**, 17119–17124.
17. Peters, N., Opherk, C., Zacherle, S., Capell, A., Gempel, P. and Dichgans, M. (2004) CADASIL-associated Notch3 mutations have differential effects both on ligand binding and ligand-induced Notch3 receptor signaling through RBP-Jk. *Exp. Cell Res.*, **299**, 454–464.
18. Joutel, A., Monet, M., Domenga, V., Riant, F. and Tournier-Lasserve, E. (2004) Pathogenic mutations associated with cerebral autosomal dominant arteriopathy with subcortical infarcts and leukoencephalopathy differently affect Jagged1 binding and Notch3 activity via the RBP/Jk signaling pathway. *Am. J. Hum. Genet.*, **74**, 338–347.
19. Low, W.C., Santa, Y., Takahashi, K., Tabira, T. and Kalaria, R.N. (2006) CADASIL-causing mutations do not alter Notch3 receptor processing and activation. *Neuroreport*, **17**, 945–949.
20. Ruchoux, M.M., Domenga, V., Brulin, P., Maciazek, J., Limol, S., Tournier-Lasserve, E. and Joutel, A. (2003) Transgenic mice expressing mutant Notch3 develop vascular alterations characteristic of cerebral autosomal dominant arteriopathy with subcortical infarcts and leukoencephalopathy. *Am. J. Pathol.*, **162**, 329–342.
21. Ihalainen, S., Soliymani, R., Iivanainen, E., Mykkänen, K., Sainio, A., Pöyhönen, M., Elenius, K., Järveläinen, H., Viitanen, M., Kalimo, H. *et al.* (2007) Proteome analysis of cultivated vascular smooth muscle cells from a CADASIL patient. *Mol. Med.*, **13**, 305–314.
22. Ellgaard, L. and Helenius, A. (2003) Quality control in the endoplasmic reticulum. *Nat. Rev. Mol. Cell Biol.*, **4**, 181–191.
23. Kleizen, B. and Braakman, I. (2004) Protein folding and quality control in the endoplasmic reticulum. *Curr. Opin. Cel. Biol.*, **16**, 343–349.
24. Zhang, K. and Kaufman, R.J. (2006) The unfolded protein response: a stress signaling pathway critical for health and disease. *Neurology*, **66**, S102–S109.
25. Zhao, L. and Ackerman, S.L. (2006) Endoplasmic reticulum stress in health and disease. *Curr. Opin. Cell Biol.*, **18**, 444–452.
26. Yoshida, H. (2007) ER stress and diseases. *FEBS J.*, **274**, 630–658.
27. Ni, M. and Lee, A.S. (2007) ER chaperones in mammalian development and human diseases. *FEBS Lett.*, **581**, 3641–3651.
28. Calloni, G., Zoffoli, S., Stefani, M., Dobson, C.M. and Chiti, F. (2005) Investigating the effects of mutations on protein aggregation in the cell. *J. Biol. Chem.*, **280**, 10607–10613.
29. Bence, N.F., Sampat, R.M. and Kopito, R.R. (2001) Impairment of the ubiquitin-proteasome system by protein aggregation. *Science*, **292**, 1552–1555.
30. Tanaka, Y., Engelender, S., Igarashi, S., Rao, R.K., Wanner, T., Tanzi, R.E., Sawa, A., Dawson, V.L., Dawson, T.M. and Ross, C.A. (2001) Inducible expression of mutant α-synuclein decreases proteasome activity and increases sensitivity to mitochondria-dependent apoptosis. *Hum. Mol. Genet.*, **10**, 919–926.
31. Kaytor, M.D., Wilkinson, K.D. and Warren, S.T. (2004) Modulating huntingtin half-life alters polyglutamine-dependent aggregate formation and cell toxicity. *J. Neurochem.*, **89**, 962–973.
32. Ravikumar, B., Acevedo-Arozena, A., Imarisio, S., Berger, Z., Vacher, C., O'Kane, C.J., Brown, S.D.M. and Rubinsztein, D.C. (2005) Dynein mutations impair autophagic clearance of aggregate-prone proteins. *Nat. Genet.*, **37**, 771–776.
33. Fujita, E., Kouroku, Y., Isoai, A., Kumagai, H., Misutani, A., Matsuda, C., Hayashi, Y.K. and Momoi, T. (2007) Two endoplasmic reticulum-associated degradation (ERAD) systems for the novel variant of the mutant dysferlin: ubiquitin/proteasome ERAD(I) and autophagy/lysosome ERAD(II). *Hum. Mol. Genet.*, **16**, 618–629.
34. Opherk, C., Duering, M., Peters, N., Karpinska, A., Rosner, S., Schneider, E., Bader, B., Giese, A. and Dichgans, M. (2009) CADASIL mutations enhance spontaneous multimerization of NOTCH3. *Hum. Mol. Genet.*, **18**, 2761–2767.
35. Trombetta, E.S. and Parodi, A.J. (2003) Quality control and protein folding in the secretory pathway. *Annu. Rev. Cell Dev. Biol.*, **19**, 649–676.
36. Okiyoneda, T., Harada, K., Takeya, M., Yamahira, K., Wada, I., Shuto, T., Suico, M.A., Hashimoto, Y. and Kai, H. (2004) Delta F508 CFTR pool in the endoplasmic reticulum is increased by calnexin overexpression. *Mol. Biol. Cell*, **15**, 563–574.
37. Free, R.B., Hazelwood, L.A., Cabrera, D.M., Spalding, H.N., Namkung, Y., Rankin, M.L. and Sibley, D.R. (2007) D1 and D2 dopamine receptor expression is regulated by direct interaction with the chaperone protein calnexin. *J. Biol. Chem.*, **282**, 21285–21300.
38. Arboleda-Velasquez, J.F., Rampal, R., Fung, E., Darland, D.C., Liu, M., Martinez, M.C., Donahue, C.P., Navarro-Gonzalez, M.F., Libby, P., D'Amore, P.A. *et al.* (2005) CADASIL mutations impair Notch3 glycosylation by Fringe. *Hum. Mol. Genet.*, **14**, 1631–1639.

39. Tsai, B., Ye, Y. and Rapoport, T.A. (2002) Retro-translocation of proteins from the endoplasmic reticulum into the cytosol. *Nat. Rev. Mol. Cell Biol.*, **3**, 246–255.
40. Friedman, J. and Xue, D. (2004) To live or die by the sword: the regulation of apoptosis by the proteasome. *Dev. Cell*, **6**, 460–461.
41. Mytilineou, C., McNaught, K.S., Shashidharan, P., Yabut, J., Baptiste, R.J., Parnandi, A. and Olanow, C.W. (2004) Inhibition of proteasome activity sensitizes dopamine neurons to protein alterations and oxidative stress. *J. Neural Transm.*, **111**, 1237–1251.
42. Bennett, E.J., Bence, N.F., Jayakumar, R. and Kopito, R.R. (2005) Global impairment of the ubiquitin-proteasome system by nuclear or cytoplasmic protein aggregates precedes inclusion body formation. *Mol. Cell*, **17**, 351–365.
43. Zinszner, H., Kuroda, M., Wang, X., Batchvarova, N., Lightfoot, R.T., Remotti, H., Stevens, J.L. and Ron, D. (1998) CHOP is implicated in programmed cell death in response to impaired function of the endoplasmic reticulum. *Genes. Dev.*, **12**, 982–995.
44. McCullough, K.D., Martindale, J.L., Klotz, L.O., Aw, T.Y. and Holbrook, N.J. (2001) Gadd153 sensitizes cells to endoplasmic reticulum stress by down-regulating Bcl2 and perturbing the cellular redox state. *Mol. Cell. Biol.*, **21**, 1249–1259.
45. Paschen, W. and Frandsen, A. (2001) Endoplasmic reticulum dysfunction—a common denominator for cell injury in acute and degenerative diseases of the brain? *J. Neurochem.*, **79**, 719–725.

Journal of Neuroimmunology 214 (2009) 93–100

Contents lists available at ScienceDirect

Journal of Neuroimmunology

journal homepage: www.elsevier.com/locate/jneuroim

Fingolimod and related compounds in a spontaneous autoimmune polyneuropathy

Hye-Jung Kim [a], Cha-Gyun Jung [a], Danuta Dukala [a], Hyun Bae [a], Rafael Kakazu [a], Robert Wollmann [b], Betty Soliven [a,*]

[a] Department of Neurology, The University of Chicago, Chicago, IL, United States
[b] Dept. of Pathology, The University of Chicago, Chicago, IL, 5841 S. Maryland Ave, Chicago, IL 60637, United States

ARTICLE INFO

Article history:
Received 6 June 2009
Received in revised form 3 July 2009
Accepted 6 July 2009

Keywords:
CIDP
Guillain–Barré syndrome
S1P receptors
NOD mice
FTY720
SEW2871

ABSTRACT

We investigated potential therapeutic effects of sphingosine-1-phosphate (S1P) receptor modulators FTY720 (fingolimod) and selective S1P1 agonist SEW2871 on a spontaneous autoimmune polyneuropathy (SAP) when given orally at 7 mo (anticipated disease onset) for 4 weeks. Clinical severity, electrophysiologic and histological findings were ameliorated in mice treated with 1 mg/kg of FTY720. Subsequent studies showed that SEW2871 was also effective in halting the progression of SAP, which was accompanied by decreased proliferative and cytokine responses to myelin protein zero (P0), and an increase in regulatory T cells. We conclude that S1P receptor modulators may play a therapeutic role in autoimmune neuropathies.

1. Introduction

Fingolimod (FTY720) is an oral S1P receptor modulator in phase III clinical trials for the treatment of multiple sclerosis (MS). A decrease in MRI and clinical disease activity was observed in a phase II study of FTY720 in MS (Kappos et al., 2006). FTY720 is highly efficacious in the MS model of experimental autoimmune encephalomyelitis (EAE) (Balatoni et al., 2007; Fujino et al., 2003; Webb et al., 2004). The beneficial effect of FTY720 in EAE is attributed to lymphocyte sequestration in secondary lymphoid organs, although it also enhances the expression of neuroregenerative genes in the CNS (Chiba et al., 1998; Foster et al., 2008; Graler and Goetzl, 2004; Mandala et al., 2002; Pinschewer et al., 2000). In addition, dynamic effects of FTY720 and related compounds in oligodendroglial lineage cells have been demonstrated (Coelho et al., 2007; Jaillard et al., 2005; Jung et al., 2007; Miron et al., 2008).

Not all treatments effective in MS also work consistently for autoimmune neuropathies such as chronic inflammatory demyelinating polyradiculoneuropathy (CIDP). For example, interferon beta (IFN-β) while effective in MS, has had contradictory outcome in CIDP (Hadden et al., 1999; Vallat et al., 2003). There is one report describing the beneficial effect of FTY720 (intraperitoneal injection) in P2-induced experimental allergic neuritis (EAN) in Lewis rats (Zhang et al., 2008). FTY720 is converted *in vivo* to FTY720-phosphate (FTY720P), which is a potent agonist of four of the five known S1P receptors (S1P1, S1P3, S1P4 and S1P5) (Brinkmann et al., 2002). It is unclear whether selective S1P1 modulators such as SEW2871 will have a similar therapeutic effect as FTY720 on EAN or EAE. T lymphocyte migration towards S1P gradient is highly dependent on S1P1 receptors, whereas dendritic cell migration is mediated primarily by S1P3 receptors (Allende et al., 2004; Maeda et al., 2007; Matloubian et al., 2004).

The goal of this study is to investigate whether FTY720 and selective S1P1 agonist SEW2871 exert a therapeutic effect in a model of spontaneous autoimmune polyneuropathy (SAP), the B7-2 knockout (KO) non-obese diabetic (NOD) mice. NOD mice are susceptible to the development of autoimmune diseases such as type 1 diabetes, thyroiditis, sialitis, or neuropathy, but disease manifestations are strongly influenced by co-stimulatory molecules and cytokine milieu (Salomon et al., 2001; Setoguchi et al., 2005). Elimination of a co-stimulatory molecule B7-2 in female NOD mice prevents type 1 diabetes and sialitis, but triggers the development of limb weakness at 6–7 mo, which progresses to quadriparesis by 8–9 mo. The incidence of neuropathy is lower in males compared to female B7-2 KO NOD mice. Unlike EAN, SAP mice do not undergo spontaneous recovery. Similar to human CIDP, electrophysiological findings in SAP are classical for a demyelinating process with superimposed axonal loss. Histological evaluation reveals the presence of inflammatory infiltrates ($CD4^+$, $CD8^+$ T cells, dendritic cells) in dorsal root ganglia and sciatic nerves but not in the CNS (Salomon et al., 2001). We and other investigators found that SAP is a Th1-mediated disease and that myelin protein zero (P0) is one of the autoantigens targeted by T cells

* Corresponding author. Dept. of Neurology MC2030, The University of Chicago, 5841 S. Maryland Ave, Chicago, IL 60637, United States. Tel.: +1 773 702 6393; fax: +1 773 9060.
E-mail address: bsoliven@neurology.bsd.uchicago.edu (B. Soliven).

0165-5728/$ - see front matter © 2009 Elsevier B.V. All rights reserved.
doi:10.1016/j.jneuroim.2009.07.006

in this model (Bour-Jordan et al., 2005; Kim et al., 2008; Louvet et al., 2009). In this study, we examined the effect of S1P receptor modulators on disease severity in SAP as determined by clinical assessment, electrophysiological, and histological evaluations. We also investigated the effect of these compounds at the level of the blood nerve barrier (BNB), on the autoreactivity to myelin P0, and on Schwann cell viability.

2. Materials and methods

2.1. Animals and reagents

All animal use procedures were conducted in strict accordance to the National Institutes of Health and University of Chicago institutional guidelines. Female B7-2 knockout (KO) NOD mice (7 mo old) were used for our studies. FTY720 (Novartis Pharma AG, Basel, Switzerland) was dissolved in distilled water. The drug was freshly prepared and given orally once daily by gavage at 0.3 to 1 mg/kg body weight. SEW2871 (Cayman chemical, MI, USA) was dissolved in dimethyl sulfoxide (DMSO) and diluted with water. SEW2871 was given orally twice a day by gavage at 10 mg/kg body weight.

2.2. Clinical and electrophysiology assessment

For clinical assessment, the following nominal scale was used: 0 – normal; 1 – flaccid tail; 2 – mild paraparesis; 3 – severe paraparesis; 4 – tetraparesis; 5 – death. Grip strength testing consisted of five separate measurements in each of two trials per session with a grip strength meter (Columbus Instruments, OH). Results of two trials were averaged for each mouse per session. After the last grip strength measurement, electrophysiologic studies of sciatic nerves were performed as described previously (Kim et al., 2008; Salomon et al., 2001). Briefly, recording needle electrodes were placed subcutaneously in the footpad. Right and left sciatic nerves were stimulated distally at the ankle and proximally at the sciatic notch using needle electrodes. Latencies, conduction velocities and peak to peak amplitudes were measured. Temperature was maintained at ≥ 30 °C during the recording. Values obtained from right and left sciatic nerves were averaged for each animal, which was then used to calculate mean $\pm$ SEM (n = number of animals).

2.3. Histological studies

Segments of the sciatic nerves were fixed in 0.5–4% paraformaldehyde, embedded in OCT compound, and snap frozen. Longitudinal sections (10 μm slices) of sciatic nerves were stained with hematoxylin–eosin (H&E), and inflammatory cells were counted at 20× magnification with tissue areas measured by image analysis. At least 3 sections were analyzed per nerve. For semithin/epon sections, nerve tissues were obtained at high sciatic levels prior to bifurcation, fixed in 4% PFA, postfixed in 1% osmium tetroxide for 1–2 h, embedded in plastic resin and stained with toluidine blue. The number of myelinated fibers over a total area of 0.09 mm^2 was counted with results expressed as % loss of myelinated fibers compared to unaffected nerves from preclinical mice. Sections were also scored using a semi-quantitative grading system: 0, normal; 1, < 25%; 2, 25–50%; 3, 51–75%; and 4 with > 75% demyelinated or thinly myelinated fibers. All histological analysis was performed in a blinded fashion.

2.4. Blood nerve barrier permeability

Evans blue albumin (EBA) solution was prepared as a mixture of 5% bovine albumin (Sigma, MO, USA) and 1% Evans blue dye (Sigma, MO, USA) in distilled water that was filtered in a PD-10 desalting column (GE healthcare, NJ, USA). B7-2 KO NOD mice were given FTY720, SEW2871 or PBS via tail vein injection. Six hours post-injection, anesthetized mice were infused with 100 μl of EBA solution through the tail vein. After 30 min, sciatic nerves were harvested and snap frozen. Longitudinal sections (10 μm) of sciatic nerves were placed on microscope slides with coverslips mounted using 50% glycerin in water. Sections were visualized using a fluorescence microscope at 10× magnification. Integrated fluorescence intensity was analyzed using the NIH Image J program. For each nerve, at least 2 areas/section for 3 sections were examined.

2.5. Splenocyte culture, proliferation and cytokine production assays

For proliferation assay, splenocytes were cultured at a density of 5×10^5 cells/well in HL-1™ medium plus non-essential amino acids (Biowhittaker), L-glutamine (2 mM), sodium pyruvate (1 mM) and β-mercaptopurine (55 μM) in flat-bottom 96 well plates, then cells were stimulated with OVA peptide (20 μg/ml), P0 peptide (20 μg/ml) or P2 peptide (20 μg/ml). On day 3, these cultures were added for 16 h with 1 μCi methyl-[^{3}H] thymidine. A stimulation index was defined by cpm in the presence of antigen divided by cpm in the absence of the antigen. Supernatants collected at 48 h from replicate cultures were assayed for IFN-γ (Endogen, Rockford, IL), IL-2, IL-10 (BD Biosciences, San Diego, CA) and IL-17 (eBioscience, San Diego, CA) using ELISA Minikits. The following peptides were used as antigens: 1) P0 (180–199) (SSKRGRQTPVLYAMLDHSRS); 2) P2 (53–78) (TESPFKNTEISFKLGQEFEETTADNR); 3) OVA (323–339) (ISQAVHAAHAEINEAGR) (GenScript Corporation, Piscataway, NJ).

2.6. Schwann cell (SC) culture and cell viability assay

Primary SCs were prepared from P3–4 rats as previously described (Iwase et al., 2005; Nagano et al., 2001). After treatment with 10 μM cytosine arabinoside (Ara C) for 48 h to eliminate proliferating fibroblasts, SCs on polylysine-coated dishes were incubated with proliferating medium: DMEM containing 10% FBS, 2 μM forskolin (fsk) and 20 μg/ml bovine pituitary extract (BPE). SCs in passages 2 and 3 were used for experiments, after removal of fsk and BPE from culture medium for at least 3 days prior to experiments. For phosphorylation studies, SCs were incubated in serum-free medium (SFM) plus insulin (5 μg/ml), transferrin (5 μg/ml) and selenium (5 ng/ml) for 24 h prior to exposure to FTY720P for 15 min. For cell viability studies, trypan blue exclusion test was used to evaluate cell death upon serum withdrawal for 3 d in the presence or absence of test agents. Detached SCs (pre and post-trypsin treatment) were centrifuged, resuspended in PBS, stained with 0.4% trypan blue and counted using a hematocytometer.

2.7. Real-time PCR

The total RNA was isolated using a Trizol reagent (Invitrogen), followed by Qiagen column purification. Real-time PCR studies were performed as described previously (Jung et al., 2007). The following primers were used: S1P1-forward (5′-CTGACCTTCCGCAAGAACATCT-3′) and reverse (5′-CTTCAGCAAGGCCAGAGACTTC-3′); S1P2-forward (5′-ACATTTCTGGAGGGCAACAC-3′) and reverse (5′-TGGTCCCCA CAGTCACAGTA-3′); S1P3-forward (5′-AGAACGAGAGCCTGTTTCCA-3′) and reverse (5′-CAG CTTCCCCACGTAATCAT-3′); S1P4-forward (5′-GGACTTCGAGGTCACTCAGC-3′) and reverse (5′-CTGCCAAACATTCATCATGG-3′); S1P5-forward (5′-CTCTAGAGCGCCACCTTACCA-3′) and reverse (5′-CCCAGCAGCAGCGACAA-3′); GAPDH-forward (5′-TTC ACCACCATGGAGAAGGC-3′) and reverse (5′-GGCATGGACTGTGGTCATGA-3′).

2.8. Western blot analysis

Cell lysis, protein count, SDS PAGE and Western blot analysis were performed as described previously (Iwase et al., 2005; Jung et al., 2007). Sample proteins (30 μg per lane) were resolved by 15% Tris–